



THE UNIVERSITY *of* EDINBURGH

Edinburgh Research Explorer

Nonphotochemical Laser-Induced Nucleation of Potassium Halides

Citation for published version:

Ward, MR, Alexander, AJ & Alexander, A 2012, 'Nonphotochemical Laser-Induced Nucleation of Potassium Halides: Effects of Wavelength and Temperature', *Crystal Growth and Design*, vol. 12, no. 9, pp. 4554-4561. <https://doi.org/10.1021/cg300750c>

Digital Object Identifier (DOI):

[10.1021/cg300750c](https://doi.org/10.1021/cg300750c)

Link:

[Link to publication record in Edinburgh Research Explorer](#)

Document Version:

Peer reviewed version

Published In:

Crystal Growth and Design

Publisher Rights Statement:

Copyright © 2012 by the American Chemical Society

General rights

Copyright for the publications made accessible via the Edinburgh Research Explorer is retained by the author(s) and / or other copyright owners and it is a condition of accessing these publications that users recognise and abide by the legal requirements associated with these rights.

Take down policy

The University of Edinburgh has made every reasonable effort to ensure that Edinburgh Research Explorer content complies with UK legislation. If you believe that the public display of this file breaches copyright please contact openaccess@ed.ac.uk providing details, and we will remove access to the work immediately and investigate your claim.



This document is the Accepted Manuscript version of a Published Work that appeared in final form in *Crystal Growth & Design*, copyright © American Chemical Society after peer review and technical editing by the publisher. To access the final edited and published work see <http://dx.doi.org/10.1021/cg300750c>

Cite as:

Ward, M. R., Alexander, A. J., & Alexander, A. (2012). Nonphotochemical Laser-Induced Nucleation of Potassium Halides: Effects of Wavelength and Temperature. *Crystal Growth & Design*, 12(9), 4554-4561.

Manuscript received: 01/06/2012; Accepted: 18/07/2012; Article published: 03/08/2012

Nonphotochemical Laser-Induced Nucleation of Potassium Halides: Effects of Wavelength and Temperature**

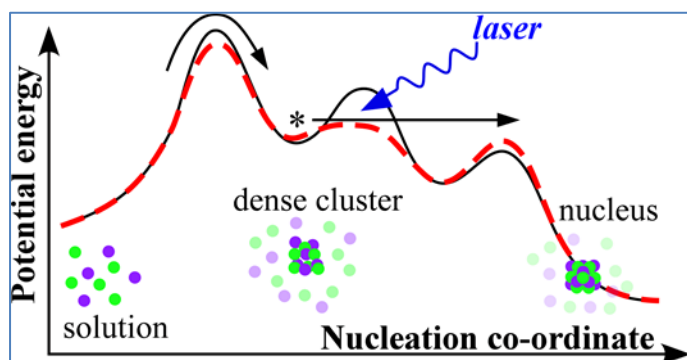
Martin R. Ward and Andrew J. Alexander*

School of Chemistry, Joseph Black Building, University of Edinburgh, West Mains Road, Edinburgh, EH9 3JJ, UK.

[*]Corresponding author; e-mail: andrew.alexander@ed.ac.uk

[**]We are grateful to Dr Philip Camp for many useful discussions, and to an anonymous reviewer for pointing out a published correction to Eq. (5). We wish to acknowledge the Science and Technology Facilities Council (STFC) and the Engineering and Physical Sciences Research Council (EPSRC) for supporting this work (EP/G067546/1), and to the Royal Society (London) for a research grant.

Graphical abstract:



Summary:

We present a detailed study of the effects of nanosecond laser pulses on laser-induced crystallization of supersaturated KCl and KBr. An electronic polarization model has been developed, which is shown to capture the essence of the nucleation mechanism. Directions for future theoretical studies of nucleation are outlined.

Abstract

Non-photochemical laser-induced nucleation (NPLIN) of KCl and KBr has been studied using nanosecond laser pulses with wavelengths of 532 and 1064 nm. The ratio of the number of samples nucleated to the number irradiated with the laser (f) follows a non-linear dependence on peak power density that approaches $f=1$ at higher incident powers, which we fit with a Poisson function. The threshold power required to nucleate samples is lower at 532 than at 1064 nm, and we observe that a higher fraction of samples nucleate when exposed to 532 nm pulses at a given laser power. In comparison to KCl, we see higher fractions of KBr samples nucleate and lower threshold values at both wavelengths. Samples of KCl of equal supersaturation at two different temperatures (23 and 33 °C) shot with 1064 nm pulses show that the 33 °C samples are significantly more labile to nucleation. The ratio of samples nucleated at 33 °C compared to 23 °C was 2.11 ± 0.47 . A classical nucleation model based on activation of sub-critical clusters in solution accounts remarkably well for the experimental data and provides phenomenological values of the crystal–solution interfacial tension (γ) at 23 °C for KCl and KBr of 5.283 and 4.817 mJ m⁻². At 33 °C the model yields a best-fit value of $\gamma = 5.429$ mJ m⁻² for KCl.

1. Introduction

Crystallization is a ubiquitous phase transition which has been exploited in the sciences as an efficient means of product separation and purification. The complex crystallization process can be considered to involve two key steps: nucleation followed by crystal growth. Of these two steps, much less is known about nucleation. The study of nucleation has been greatly hindered because of the stochastic nature of the process. It is well known that nucleation of a metastable sample can be induced by physical perturbations such as rapid cooling, mechanical shock, sonication, or seeding.¹ One particularly intriguing method is nucleation by the action of light. Light with sufficiently high photon energies can create nucleation centres photochemically; this effect was the basis for the pioneering work of John Tyndall.² Alternatively, light can be used to cause nucleation photomechanically, e.g., by ablation or cavitation.³⁻¹⁴ Other methods include optical trapping or optically biased diffusion.¹⁵⁻²² Recently, non-photochemical laser-induced nucleation (NPLIN) has been demonstrated, in which case there is no photochemical damage to the sample;^{23, 24} this effect has the potential to enable direct measurements of a nucleation process analogous to homogeneous nucleation.

In the first study of NPLIN by Garetz *et al.*, it was observed that supersaturated aqueous solutions of urea were nucleated upon exposure to trains of near-infrared (1064 nm) laser pulses (20 ns pulses, ~ 0.1 J pulse⁻¹).²³ The group explained the effect using a model based upon the nonlinear optical Kerr effect (OKE) whereby the incident electric field induces alignment of molecular units within

clusters.²⁵ It was proposed that the solute molecules, contained within precursor clusters in solution, are reorganized into a more-ordered state through which nucleation may proceed. Interestingly, it was noted that it was necessary to age supersaturated samples for a period of at least a few days prior to shooting; it was suggested that the ageing time allowed precursor clusters to grow sufficiently large for NPLIN to occur. The requirement for sample ageing was reinforced by subsequent work on glycine,²⁵⁻²⁷ hen egg-white lysozyme (HEWL),²⁸ and l-histidine.²⁹ Theoretical simulations by Knott *et al.*, however, suggest that the free energy gain from the orientational bias at the electric field strengths involved are not sufficient to explain NPLIN by the OKE mechanism.³⁰

Alexander and co-workers have studied NPLIN of a number of metastable systems,^{31, 32} in particular the benchmark system of aqueous potassium chloride (KCl).^{24, 33, 34} It was demonstrated that samples of KCl with supersaturations ($S = C/C_{\text{sat}}$) in the range 1.05–1.10 can be nucleated by a single pulse from a nanosecond laser. The probability of nucleation was found to be linearly dependent on the power density of the laser pulse. It was noted that there was a minimum laser power density (a threshold) required to nucleate samples. On account of the simple cubic structure which crystalline KCl assumes, there are no molecular units to be aligned as envisaged by the OKE mechanism, and no polarization dependence was observed. A different nucleation mechanism was proposed, based on the electronic polarization of precursor clusters induced by the transient electric fields of the laser pulse.²⁴ The results were modelled using a modified classical nucleation theory (CNT).

The aqueous KCl system offers several advantages over systems such as urea or glycine for systematic studies of NPLIN. Because a single laser pulse can nucleate a single crystal, the critical point for nucleation must occur within the duration (~10 ns) of the laser pulse. Also, it was found that samples of KCl do not require ageing beyond the cooling time required to achieve supersaturation, making sample preparation easier.

Recent studies have indicated a clear need to provide more data in order to develop and test models of NPLIN.^{24, 31, 35-37} To move towards fulfilling this need, we have extended our work on the potassium halide system to investigate the effects of wavelength, temperature and anion (Br^- versus Cl^-). We find that general trends of the results fit well with our modified CNT model; however, several features of NPLIN have yet to be accounted for.

2. Experimental methods

Supersaturated solutions were prepared by dissolution of KCl (puriss, > 99%, Fluka) and KBr (puriss, Sigma) in deionized water (Chromanorm HPLC grade, VWR). The saturation concentrations (C_{sat}) of KCl and KBr in aqueous solution at 23.0 °C are 4.688 and 5.610 mol kg⁻¹, respectively.³⁸ Solutions

were prepared at a supersaturation ($S = C / C_{\text{sat}}$) of 1.060. The sample solutions were syringe-filtered while hot (0.22 μm , Millex-GP) into clean cylindrical glass vials (20.3 mm diameter) with screw-caps (sample volume $\sim 3.8 \text{ cm}^3$). The vials used were cleaned with detergent and rinsed several times, the final rinsing with syringe-filtered deionized water. Approximately 20 sample vials were prepared for each sample. All samples were first recrystallized before going through a heating, cooling and irradiation cycle. Nucleated samples were regenerated by heating on a hotplate (50 $^{\circ}\text{C}$) with regular shaking followed by brief ultrasonication in a water bath (40 $^{\circ}\text{C}$). Dissolved samples were then transferred to a temperature-controlled water bath (23.0 $^{\circ}\text{C}$) for a period of 40 minutes. We have observed that samples that do not nucleate during the 40 minute cooling period are stable, typically for several days or more. We note that ageing of samples beyond the time for cooling does not appear to be necessary for potassium halide systems,²⁴ but has been reported to be critical for larger molecules.^{23, 26}

Samples were shot with the laser by placing the cooled sample vials in the beam path and exposing each to a single pulse of laser light with wavelengths of 1064 or 532 nm (Brilliant Nd³⁺:YAG, Quantel); see Fig. 1. The linearly polarized laser light was passed through an iris (5.5 mm diameter) and then through a Glan–Laser polarizer. The polarizer allows fine control over the power of the beam *via* Malus’s law, and ensures purity of the final linear polarization. The vial acts as a cylindrical lens, loosely focussing the beam in one direction only as shown in Fig. 1. The mean laser power of the unfocussed beam was recorded using a power meter (Nova, Ophir) and the value converted to peak power density (j_{peak}) by taking into account the duration of the laser pulse (5.3 ns at 532 nm, 6.3 ns at 1064 nm) and the area of the beam at the exit of the vial. The focussing depends on the refractive index of the solution at a given wavelength (see Table A1 in the Appendix). With an input area of 0.24 cm^2 , the area of the beam at the exit of the sample vial was calculated to be $\sim 0.11 \text{ cm}^2$. The experiments were conducted in the range of peak power densities 5–42 MW cm^{-2} (approximately 3–30 mJ pulse^{-1} of the unfocussed beam, depending on wavelength). There was no evidence of bubble production during irradiation. Immediately after shooting, samples were returned to the temperature-controlled water bath. After a period of 15 minutes some samples showed the presence of one or more crystals in the bottom of the sample vial. The locations of the fallen crystals indicated that they can form at any point along the beam path through the solution. The fraction of samples that had nucleated ($f = n / N$) was calculated as the ratio of the number of samples showing crystals (n) to the number shot (N). In previous work the experimental fraction was measured by cumulative measurements at increasing laser powers;²⁴ in the present work, each data point represents measurements carried out at a fixed laser power. Approximately 80 samples were shot at each power. Single standard deviations were calculated from repeat measurements on batches of 20 vials at each laser power.

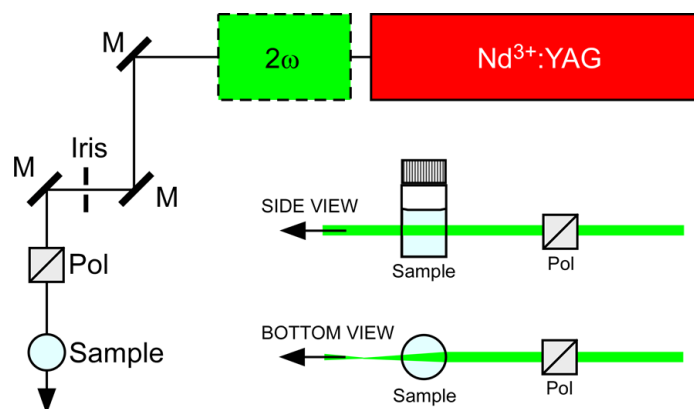


Fig. 1. Schematic layout of the experimental setup for laser-induced nucleation. The Nd³⁺:YAG laser outputs pulses of 1064 nm light; these may be frequency doubled to 532 nm by inserting a second-harmonic generation module (2ω). Coated mirrors (M) were used to steer the beam. The diameter of the input beam was 5.5 mm (selected by the iris), and was delivered through the centre of the sample, as illustrated.

The effects of temperature were studied by comparing nucleation in solutions of KCl with $S = 1.060$ at 33 °C to those with the same S but at 23 °C. The solubility of KCl in aqueous solution at 33 °C is 5.092 mol kg⁻¹.³⁸ Sample vials were prepared and handled following the same procedures as outlined above. In order to maintain temperature during the shooting process, a brass sample holder was used, which was heated by ceramic heating cartridges via a programmable temperature controller (2132, Eurotherm). The samples were individually seated in the block for a period of 60 seconds prior to shooting. The sample was shot with a single pulse of linearly polarized 1064 nm laser light, following which the sample was returned to the water bath at 33 °C. The fraction of samples nucleated (f) was counted after 15 minutes. The process was repeated for different laser power densities in the range 9–20 MW cm⁻².

Over the course of the experiments it was observed that KBr nuclei always grew in the same crystal habit, forming rough-edged square crystals. On the other hand KCl was seen to produce several different shapes, occasionally exhibiting single crystals in different habits in a single nucleated sample. Aside from the typical square crystals, as seen with KBr, we see curved columnar-like crystals and extremely thin, high quality, square crystals. There was no apparent correlation between the crystal shape and incident power or number of crystals produced per nucleated sample. During the experiments the numbers of crystals produced in a nucleated sample were counted. Accurate counts were not always possible due to multiple nuclei forming conglomerates during crystal growth, however a trend was clearly observed. The mean numbers of crystals produced were seen to increase with incident laser power with one crystal being produced consistently at low laser powers.

3. Results

Plots of the fraction of samples nucleated (f) versus peak power-density (j_{peak}) for KCl and KBr samples are shown in Figs 2(a) and 2(b). The low-power portion of each set of data is seen to be approximately linear. The slope is a measure of how labile the samples are to nucleation; we will refer to the magnitude of this slope as the *lability* of the samples. Lability is therefore a measure of how susceptible a solution is to NPLIN; higher lability means more likely to nucleate. All of the data sets show a distinct threshold at low peak-power densities, as has been seen in several other systems. At higher peak power densities it can be seen that the data curve towards a plateau near $f=1$. It may appear at first that this curve is indicative of a non-linear mechanism at higher powers: however, we note that the experiments count samples nucleated, not the number of nuclei. To fit the data, we use a Poisson distribution,

$$p(n) = \frac{\lambda^n e^{-\lambda}}{n!}, \quad (1)$$

where $p(n)$ is the probability of obtaining n nuclei in a sample, and λ is the mean number of nuclei produced by a given laser power density. Since the total probability sums to unity, the probability of obtaining *at least* 1 nucleus is thus $1 - p(\text{no nuclei})$, i.e.,

$$p(n \geq 1) = 1 - p(0) = 1 - e^{-\lambda}. \quad (2)$$

For the polarization nucleation model, we show later (Appendix A) that the mean number of nuclei depends linearly on peak laser power density, $\lambda = m(j_{\text{peak}} - j_0)$, where j_0 represents the low-power threshold and m is the lability. Therefore we can fit the experimental fraction of samples nucleated with the following function,

$$f(j_{\text{peak}}) = 1 - \exp[-m(j_{\text{peak}} - j_0)]. \quad (3)$$

Near to the threshold (as $j_{\text{peak}} \rightarrow j_0$) to first-order in Eq. (3) we find $f(j_{\text{peak}}) = m j_{\text{peak}}$; in other words, the fraction of samples that nucleate is directly proportional to laser power density, as we observe in the experiments.²⁴

The experimental data were fitted using Eq. (3) by a non-linear least squares method, and the values of the parameters obtained are summarised in Table 1. The results show that KBr is more labile than KCl under equivalent conditions, with a correspondingly lower power threshold. It can also be seen that 532 nm laser light is more effective than 1064 nm light at inducing NPLIN, and that the thresholds are lower at 532 nm. The threshold value for KCl at 1064 nm reported here ($8.2 \pm 0.5 \text{ MW cm}^{-2}$) is slightly higher than reported previously ($6.4 \pm 0.5 \text{ MW cm}^{-2}$),²⁴ which we attribute to the use of a linear-fit function in the previous work.

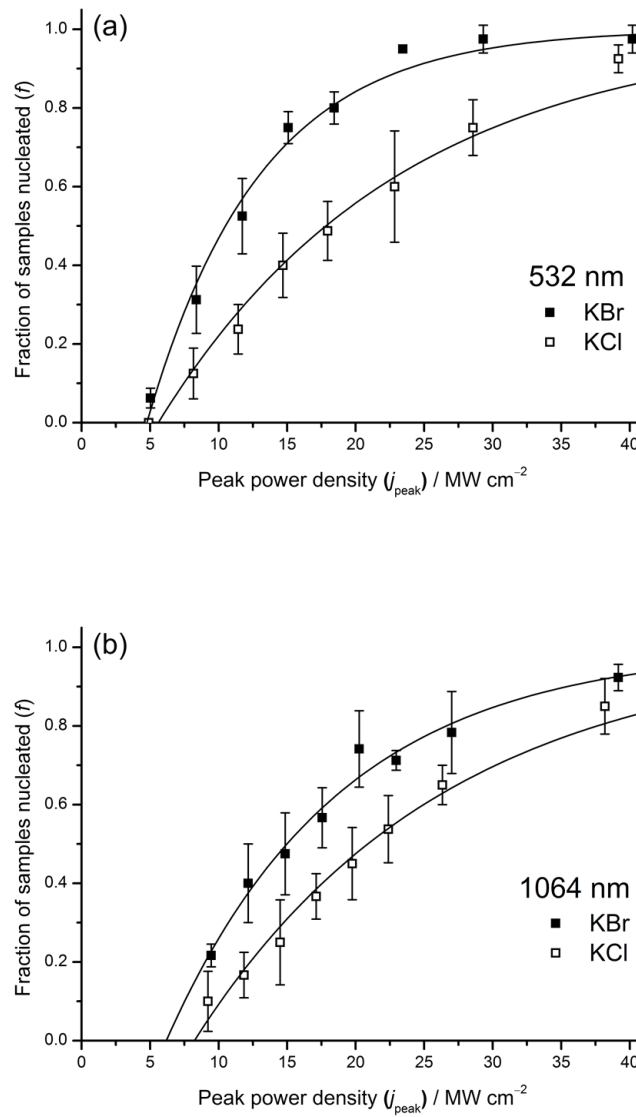


Fig. 2. Plots of fraction of samples nucleated at 23 °C with a single laser pulse against peak laser power density at different wavelengths: (a) 532 nm, and (b) 1064 nm. Solid squares represent KBr, open squares represent KCl. Error bars represent single standard deviations from 4 repeat measurements on 20 samples at each point (N.B., the fraction of samples nucleated is not obtained cumulatively with increasing power). Poisson function fits to the data are shown as solid lines; labilities and thresholds obtained are listed in Table 1.

Temperature / °C	Wavelength (Λ) / nm	Solute	Threshold peak power density (j_0) / MW cm ⁻²	Lability (m) / cm ² MW ⁻¹
23	532	KBr	4.8 ± 0.3	0.121 ± 0.009
23	532	KCl	5.6 ± 0.5	0.057 ± 0.004
23	1064	KBr	6.2 ± 0.7	0.079 ± 0.006
23	1064	KCl	8.2 ± 0.5	0.055 ± 0.003
33	1064	KCl	7.7 ± 1.1	0.115 ± 0.025

Table 1. Threshold peak power densities and labilities for NPLIN of aqueous KCl and KBr at different laser wavelengths and temperatures. Supersaturation, $S = 1.060$ for all samples (N.B., the concentration of KCl at 33 °C is higher than that at 23 °C). The parameters were obtained by fitting the data shown in Figs 1 and 2 using Eq. (3): see text for details.

Plots of the fraction of KCl samples nucleated versus peak power density for equivalent supersaturation ($S = 1.060$) at 23 and 33 °C are shown in Fig. 3. The corresponding fits from the Poisson function (Eq. 3) are summarized in Table 1. Comparing the two plots we see that the samples at 33 °C are significantly more labile than those at 23 °C. The ratio of labilities, for 33 °C versus 23 °C, is 2.11 ± 0.47 . The threshold power densities are similar, suggesting that both sample sets share a common threshold value.

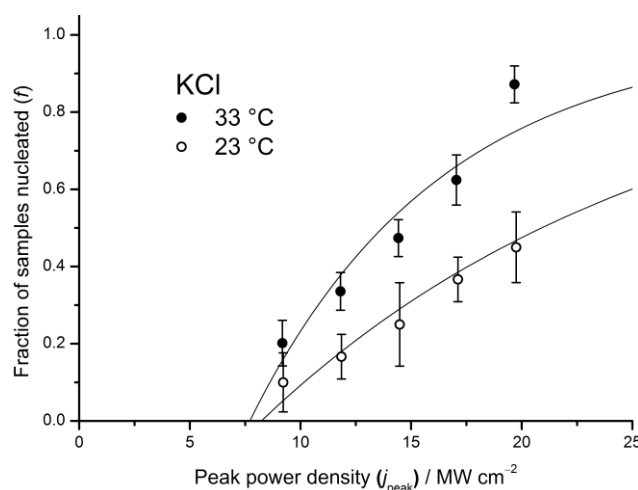


Fig. 3. Plots of fraction of KCl samples nucleated against peak laser power density for equivalent supersaturations ($S = 1.060$) at different temperatures. Solid circles represent data at 33 °C, open circles at 23 °C. Error bars represent single standard deviations from 4 repeat measurements on 20 samples at each point (N.B., the fraction of samples nucleated is not obtained cumulatively with increasing power). Poisson function fits to the data are shown as solid lines; labilities and thresholds obtained are listed in Table 1.

4. Discussion

The results show that 532 nm laser pulses are more effective than 1064 nm pulses at causing NPLIN. This trend matches the observations of Garetz *et al.* for aqueous urea solutions.³⁹ In the urea study, trains of several hundred pulses were used; sample heating during irradiation at 1064 nm was identified as the probable cause of the higher threshold power value observed at 1064 nm. In our experiments, however, the laser power densities used are an order of magnitude smaller, and more importantly, only single laser pulses were used to induce nucleation. For KBr, we estimate the local heating in the volume illuminated to be $\sim 6 \times 10^{-5}$ °C at 532 nm, and $\sim 14 \times 10^{-3}$ °C at 1064 nm: the values for KCl are slightly lower. These temperature increases are entirely negligible.³³

During the course of the experiments it was observed that KBr samples generally yielded more crystals than KCl samples at equivalent laser powers. Both KBr and KCl form centrosymmetric cubic crystal structures in the experimental conditions of the present work. At $S = 1.060$, the concentrations were $C = 5.947$ mol kg⁻¹ (KBr) and 4.969 mol kg⁻¹ (KCl). KBr samples have 20% more solute ions, but the increase in lability for KBr relative to KCl is much greater (by a factor of 2 at 532 nm), suggesting that the nature of the anion wields a more subtle influence on NPLIN. Similarly, for the effects of temperature on KCl, the absolute concentrations were 4.969 and 5.398 mol kg⁻¹ at 23 and 33 °C, respectively, i.e., a difference of 9%; however, the lability increases by a factor of 2, so differences in concentration cannot be the sole cause.

As discussed in detail elsewhere,^{24, 31, 34} we have developed a modified classical nucleation model of NPLIN. The model is based on the electrostatic result that the free energy of a dielectric particle in a medium of lower permittivity is reduced in the presence of a homogeneous electric field. We assume that there is a population of sub-critical clusters, some of which become activated to become nuclei by the electric field of the laser pulse. This activation occurs through electronic polarization of the cluster. The free energy of a cluster can be written²⁴

$$\Delta G(r, E) = 4\pi r^2 \gamma - \frac{4}{3} \pi r^3 (A \ln S + aE^2) \quad (4)$$

In this equation, r is the radius of a sub-critical cluster, γ is the solution–solute interfacial tension, S is supersaturation, and E is the electric field strength. The parameters A and a depend upon physical properties of the solute, solvent and the light, as detailed in Appendix A. To calculate the number of nuclei produced in the volume of the solution irradiated by the laser pulse (N_{nuc}) we assume a Boltzmann distribution of cluster sizes based on Eq. (4), as outlined in the Appendix. We stress that our revised model presented here returns absolute numbers of nuclei produced; our previous work on KCl in solution was a preliminary model that required a scaling parameter to fit the data.²⁴ As demonstrated in the Appendix, we find that N_{nuc} depends linearly on j_{peak} , but with a zero threshold

(i.e., $j_0 = 0 \text{ MW cm}^{-2}$). Model values for the lability (m) were obtained by calculating N_{nuc} as outlined in the Appendix.

The key parameter that is undetermined in our model is the solution–solute interfacial tension, γ . This value is independent of the wavelength used for NPLIN, but is expected to depend on temperature. The model was used to find the value of γ that fits the experimental values of lability at 1064 nm, as shown in Table 2. As a test of performance of the model, the value of γ obtained was then used to calculate the lability at 532 nm. As can be seen in Table 2, the model lability at 1064 nm is lower than that at 532 nm, which reproduces the experimental trend, but the model underestimates the *magnitude* of difference between the wavelengths for KBr. For KCl, the agreement between model and experiment is quite good, reproducing both the trend and the magnitude of the lability.

In our model, the relative permittivity of the solid phase (ϵ_s) is a major factor that controls the polarization of clusters (the term in aE^2 in Eq. 4). Looking at Table A1, we see ϵ_s of KCl at 532 nm is larger than at 1064 nm. Likewise, the relative permittivity of KBr is greater than KCl. This trend in permittivity matches the trend in experimental lability, and gives a direct physical insight into the effect of cluster polarization on NPLIN.

The value of interfacial tension for KCl at 1064 ($\gamma = 5.283 \text{ mJ m}^{-2}$) is higher than that obtained from our previous model ($\gamma = 2.19 \text{ mJ m}^{-2}$).²⁴ This difference can be attributed to several factors: (1) improvement in the quality of data (80 samples each at 8 power densities, rather than 30 samples cumulatively); (2) fitting the experimental data with a more appropriate function (the Poisson model, Eq. 3); (3) refinement of the theoretical model so that it does not rely on an arbitrary scaling factor (Appendix A).

	Lability (m) / $\text{cm}^2 \text{MW}^{-1}$				Interfacial tension (γ) / mJ m^{-2}	
	Experiment		Model		Model	Theory ⁴⁰
	532 nm	1064 nm	532 nm (predicted)	1064 nm (fitted)	1064 nm (fitted)	
KBr	0.121	0.079	0.083	0.079	4.817	19.52
KCl (23 °C)	0.057	0.055	0.056	0.055	5.283	24.99
KCl (33 °C)		0.115		0.115	5.429	24.90

Table 2. Experimental and model labilities of potassium halide samples for NPLIN at two wavelengths (see Table 1). The experimental results at 1064 nm were fitted to obtain the model value of the interfacial tension (γ) shown; the model value of γ was then used to predict the lability at 532 nm. Overall, the model predicts the correct trends with respect to wavelength and solute. Theoretical values (right-hand column) were obtained using the Mersmann equation (Eq. 5).⁴⁰⁻⁴²

For KBr we obtain $\gamma = 4.817 \text{ mJ m}^{-2}$, and for KCl we find $\gamma = 5.283 \text{ mJ m}^{-2}$. These values are of the right magnitude expected for highly soluble salts.⁴¹ There is a large spread of values for γ in the literature (0.98–163 mJ m^{-2}):⁴³ this can be attributed to the variability of experimental techniques and conditions employed. For sources that give values for both KCl and KBr,^{41, 43, 44} it was found that $\gamma(\text{KCl}) > \gamma(\text{KBr})$, in agreement with the trend seen here. For KCl at 33 °C, we find that $\gamma = 5.429 \text{ mJ m}^{-2}$ reproduces the experimental lability: this is 2.8 % higher than γ at 23 °C, and is close to the ratio of temperatures ($306.15/296.15 = 1.034$). Mersmann calculated a simple expression for solution interfacial tension based on thermodynamics;⁴⁰ after correction to assume spherical instead of cubic-shaped clusters, this is written as^{41, 42}

$$\gamma = \frac{2}{6^{1/3}} k_B T \left(\frac{\rho_s N_A}{\pi M} \right)^{2/3} \ln \frac{\rho_s}{w \rho_L}, \quad (5)$$

where k_B is Boltzmann's constant, T is temperature, M is the molar mass of the solute, N_A is the Avogadro constant, w is the mass fraction of solute in the solution, and ρ_s and ρ_L are the densities of the solid and solution, respectively. In this equation, the values of the parameters for the saturated solution were used. The values calculated from Eq. 5 are given in the right-hand column of Table 2. As can be seen, these are a factor of 4–5 larger than our model values. The higher lability at 33 °C is not reproduced by the theory: although Eq. 5 shows that $\gamma \propto T$, there are additional effects from concentration incorporated in the other terms.

Our nucleation model does a good—in fact, remarkable—job of reproducing the experimental data. Why remarkable? For one thing, the model is fed only by simple bulk physical data for the solid and

solute. For another, we are placing quite a heavy responsibility on a single parameter, the interfacial tension. For example, the interfacial tension is expected to depend on cluster size and structure, which our model does not include. Finally, the model tells us nothing about the internal dynamics of the cluster that cause it to become critical during the presence of the laser field.

The main ingredient that is missing from the model is *structure*, which is the basis for the so-called 2-step model for homogeneous nucleation.^{45, 46} We consider the following sequence (see Fig. 4): (1) the solution matures to form a distribution of clusters with variable sizes, structures and compositions; (2) while the field is present, a candidate cluster reorganizes to become super-critical. In step (1), solute ions can aggregate over time to become clusters; in the 2-step model of nucleation these are suggested to be dense, liquid-like clusters.⁴⁷ The strongest evidence for these clusters has come from protein crystallization, but simulations indicate that this cluster pathway to nucleation should be favorable for most systems.⁴⁸⁻⁵¹

We expect the dense potassium halide clusters to be disordered and defective by comparison to the crystalline solid, possibly retaining one or more solvent molecules $[K^+_x X^-_y]^{x-y}(H_2O)_z$.⁵² We can think of a suitable cluster being on a multi-dimensional potential energy surface, where the number of co-ordinate parameters (such as bond lengths and angles) is $\sim 3N$ (where N is the total number of ions and solvent molecules). The polarizability of the cluster changes with its internal structure. Prior to nucleation, the cluster is essentially trapped in a local minimum on this surface (Fig. 4). For step (2), the E -field modifies *preferentially* the potential energy of one exit channel from this local minimum; allowing it to gain access to new structures where it may then become super-critical, and nucleation may ensue. Compared to the sketch in Fig. 4, there may be many barriers in different directions on the potential energy surface: all that is required is one structure co-ordinate that is more susceptible to the E -field. After being released from the metastable dense-cluster configuration, it may have sufficient kinetic energy to pass additional local minima and barriers.

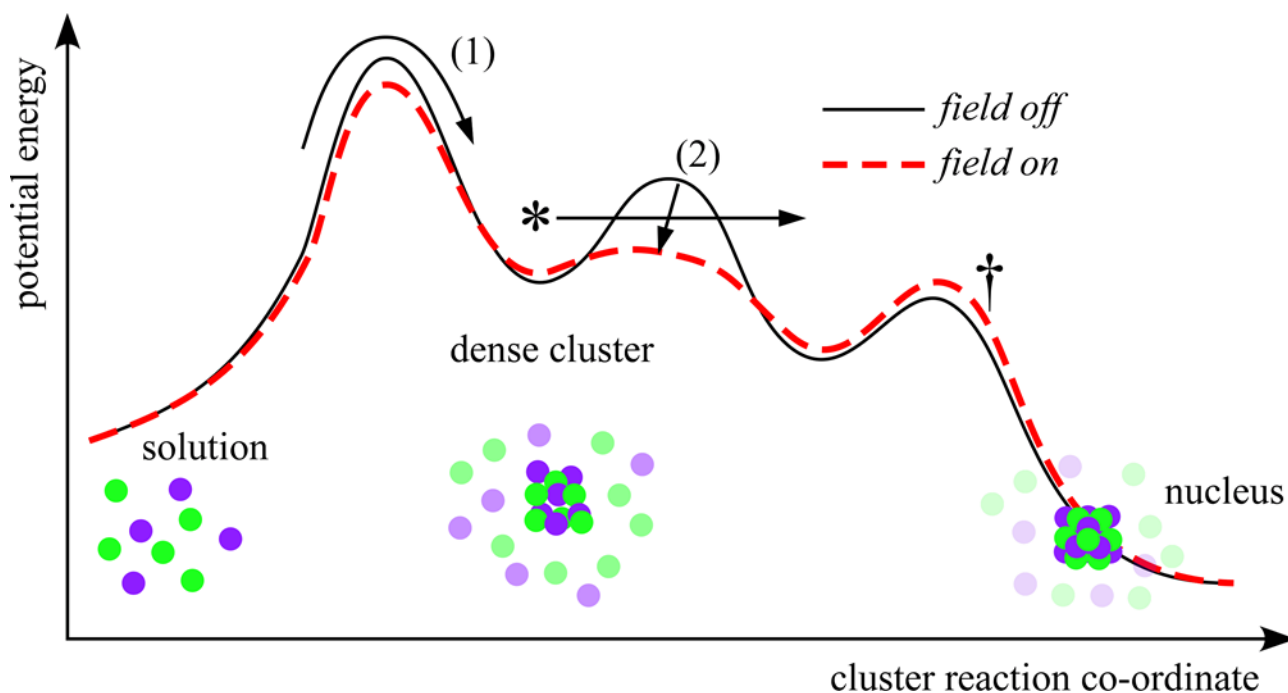


Fig. 4. Schematic diagram illustrating the transition (1) of a cluster from being loosely associated in solution to a dense cluster (*), and finally to become a nucleus due to the electric field (E) of the laser pulse (2). The curves represent the potential energy for a candidate cluster in zero-field ($E = 0$, black solid line) and high-field ($E > 0$, red dashed line). The dense cluster is considered to be non-crystalline or glass-like and may contain one or more H_2O molecules. The local potential barrier at the right (†) represents further topology for which the nucleus has sufficient energy to cross, once it is released from the dense-cluster configuration. Green circles represent chloride anions, purple circles represent sodium cations; water molecules surround the ions, but have been omitted for clarity.

One of the appealing features of the 2-step NPLIN mechanism is the timescale for step (2): since the cluster is already quite dense, only relatively small changes in co-ordinates are required to achieve criticality. The timescale for short-range motion of ion pairs is estimated to be ~ 1 ps,⁵³ which is sufficiently short for many periods of motion to occur during the ~ 5 ns of the laser pulse. We would expect the period for collective motion of larger groups of ions to be one or two orders of magnitude longer, ~ 100 ps. The concept of this rapid transition from a defective cluster to a nucleus has been proposed before. In studies of crystalloluminescence (luminescence due to crystallization) of NaCl, Garten and Head observed point pulses of light that correlated quantitatively with the number of crystals nucleated.^{54, 55} After considering the energies and concentrations involved, they concluded “... *that the primary excitation energy is derived from a phase change, indicating that the critical nucleus which forms by diffusion as a disordered quasi-liquid or glass-like aggregate eventually ‘clicks’ into crystalline form in less than 8×10^{-8} sec.*”. The timescale quoted was limited by the photodetector: after further work this was revised to less than 5 ns.

Finally, it is worth considering the direction for revised models of nucleation in general, and NPLIN in particular. The physics of the interaction between the electric field of the laser pulse and the polarizability could be applied to a revised, 2-step model. The main stumbling block, however, is an understanding of the structure of the solution, i.e., details of the metastable dense-cluster phase, and the population of clusters extant. Therefore, further experimental and theoretical work is needed to improve our knowledge of step (1) of the 2-step model of nucleation.

5. Conclusions

In conclusion, we have studied the effects of temperature and wavelength on the non-photochemical laser-induced nucleation (NPLIN) of KBr and KCl from supersaturated aqueous solution. Samples exposed to 532 nm pulses consistently demonstrate a higher sample lability and lower threshold power to nucleation compared to those shot with 1064 nm pulses. Further experiments were carried out in which KCl samples of equal supersaturation (1.060) at two different temperatures (23 and 33°C) were shot with single pulses of 1064 nm light. The results suggest that both sets of samples share a common threshold power to nucleation, with the samples prepared for 33 °C demonstrating a significantly higher lability than those at 23 °C. The results were analysed using a model based on the polarization of sub-critical clusters in solution, which provides a remarkably good description of the probability of nucleation occurring as a function of incident peak power density and solute used. It is hoped that these results will provide the basis of further experimental and theoretical work that is required in order to better understand the dynamics and mechanism responsible for NPLIN, and crystal nucleation in general.

Appendix A

From Eq. (4), the critical radius of a cluster—the size where it becomes a nucleus—is given by²⁴

$$r_c(E) = \frac{2\gamma}{A \ln S + aE^2}, \quad (\text{A1})$$

with $A = \frac{\rho_s RT}{M}$, where ρ_s is the density of the solid, R is the gas constant, T is temperature, and M is the molar mass. In terms of the peak laser power density (j_{peak}), the electric field (E) can be written

$$E = \sqrt{\frac{2j_{\text{peak}}}{c\epsilon_0}}, \quad (\text{A2})$$

where c is the speed of light in vacuum, and ϵ_0 is the electric constant. The electrostatic energy term is given by

$$aE^2 = \frac{3j_{\text{peak}}\epsilon_L}{c} \left(\frac{\epsilon_s - \epsilon_L}{\epsilon_s + 2\epsilon_L} \right), \quad (\text{A3})$$

where ϵ_L is the permittivity of the liquid solvent (water) and ϵ_s is the permittivity of the solid. The classical nucleation model can be employed to calculate the number of nuclei (N_{nuc}) produced in the sample volume irradiated by the laser for an aqueous solute. Writing Eq. A8 of ref. 31 in terms of the radius r of a spherical cluster, we have

$$N_{\text{nuc}} = N_{\text{molec}} \cdot \frac{3M}{4\pi N_A \rho_s} \cdot \frac{I_1}{I_2}, \quad (\text{A4})$$

where N_A is the Avogadro constant. The integrals I_1 and I_2 are given as follows:

$$I_1 = \int_{r_c(E)}^{r_c(0)} e^{-\beta \Delta G(r,0)} dr, \quad (\text{A5})$$

$$I_2 = \int_0^{r_c(0)} r^3 e^{-\beta \Delta G(r,0)} dr. \quad (\text{A6})$$

where $\beta = (1 / k_B T)$, k_B is the Boltzmann constant, and $\Delta G(r, E)$ is given by Eq. (4). N_{molec} is the number of potassium halide (KX = KCl or KBr) ion-pairs in the volume illuminated by the laser (V ,

which we estimate by a simple ray-tracing procedure). Substituting for N_{molec} in terms of the mass fraction of solute, $w = m_{\text{KX}} / (m_{\text{KX}} + m_{\text{H}_2\text{O}})$, we have

$$N_{\text{nuc}} = \frac{3wV\rho_{\text{L}}}{4\pi\rho_{\text{S}}} \cdot \frac{I_1}{I_2} \quad (\text{A7})$$

We calculate Eq. (A7) by numerical integration of the integrals I_1 and I_2 , using the physical parameters for KCl and KBr summarized in Table A1. We identify N_{nuc} as the model value of the Poisson parameter (λ). From the limits of the integral in Eq. A4, we see that $N_{\text{nuc}} = 0$ at $E = j_{\text{peak}} = 0$,

so the model labilities (m) can be calculated as $m = \frac{N_{\text{nuc}}}{j_{\text{peak}}}$; the results of model calculations are given in Table 2 in the main text.

It can be shown that the model reproduces the expected linear dependence of N_{nuc} on peak laser power density as follows. The only dependence of N_{nuc} on E is contained entirely in integral I_1 , since I_2 does not depend on E . To first order in E^2 , the lower limit of the integral can be written

$$r_c(E) \approx r_c(0) \left[1 - \frac{aE^2}{A \ln S} \right] = r_c(0) - \delta r, \quad (\text{A8})$$

where $\delta r = \frac{2\gamma a E^2}{(A \ln S)^2}$ (with $A \gg a$). For the integral I_1 ,

$$I_1 = \int_{r_c(0) - \delta r}^{r_c(0)} f(r) \, dr = f(r) \delta r. \quad (\text{A9})$$

Then we have

$$N_{\text{nuc}} = \frac{3wV\rho_{\text{L}}}{4\pi\rho_{\text{S}}} \cdot \frac{e^{-\beta \Delta G(r_c(0), 0)}}{I_2} \cdot \frac{2\gamma a E^2}{(A \ln S)^2} \propto E^2, \quad (\text{A10})$$

in other words, $N_{\text{nuc}} \propto j_{\text{peak}}$.

Parameter		KCl (23 °C)	KBr (23 °C)	KCl (33 °C)
molar mass (M) / 10^{-3} kg mol $^{-1}$		74.55	119.0	74.55
molality (C) / mol kg $^{-1}$		4.969	5.947	5.398
solute mass fraction (w)		0.2703	0.4144	0.2869
solution density (ρ_L) / kg m $^{-3}$		1176	1375	1184
solid density (ρ_S) / kg m $^{-3}$		1984	2750	1984
relative permittivity, solid (ϵ_S)	532 nm	2.230	2.455	—
	1064 nm	2.189	2.384	2.188
relative permittivity, water (ϵ_L)	532 nm	1.783	1.783	—
	1064 nm	1.754	1.754	1.751
solution refractive index (n_L)	532 nm	1.365	1.376	
	1064 nm	1.352	1.363	1.351
volume irradiated (V) / 10^{-6} m 3	532 nm	0.3451	0.3424	—
	1064 nm	0.3482	0.3455	0.3487

Table A1. Parameters employed in the modified classical nucleation model of NPLIN used in the present work.⁵⁶ Where appropriate, values are given for the supersaturation $S = 1.060$ (for C , w , ρ_L , V). The irradiated volume was calculated using a ray tracing procedure to account for the slight focussing in the vial; the volumes for each solution and laser wavelength differ due to differences in the solution refractive indices.

References

- (1) Mullin, J. W., *Crystallization*. 4th ed.; Butterworth-Heinemann: Oxford, 2001.
- (2) Tyndall, J., On a New Series of Chemical Reactions Produced by Light. *Proc. Roy. Soc. London* **1868-1869**, 17, 99-102.
- (3) Soare, A.; Dijkink, R.; Pascual, M. R.; Sun, C.; Cains, P. W.; Lohse, D.; Stankiewicz, A. I.; Kramer, H. J. M., Crystal Nucleation by Laser-Induced Cavitation. *Cryst. Growth Des.* **2011**, 11, (6), 2311-2316.
- (4) Adachi, H.; Takano, K.; Hosokawa, Y.; Inoue, T.; Mori, Y.; Matsumura, H.; Yoshimura, M.; Tsunaka, Y.; Morikawa, M.; Kanaya, S.; Masuhara, H.; Kai, Y.; Sasaki, T., Laser irradiated growth of protein crystal. *Jap. J. Appl. Phys.* **2003**, 42, L798.
- (5) Hosokawa, Y.; Adachi, H.; Yoshimura, M.; Mori, Y.; Sasaki, T.; Masuhara, H., Femtosecond laser-induced crystallization of 4-(dimethylamino)-N-methyl-4-stilbazolium tosylate. *Cryst. Growth Des.* **2005**, 5, (3), 861-863.
- (6) Yoshikawa, H. Y.; Hosokawa, Y.; Masuhara, H., Spatial control of urea crystal growth by focused femtosecond laser irradiation. *Cryst. Growth Des.* **2006**, 6, (1), 302-305.
- (7) Nakamura, K.; Hosokawa, Y.; Masuhara, H., Anthracene crystallization induced by single-shot femtosecond laser irradiation: Experimental evidence for the important role of bubbles. *Cryst. Growth Des.* **2007**, 7, (5), 885-889.
- (8) Okutsu, T., Photochemically-induced crystallization of protein. *J. Photochem. Photobiol. C* **2007**, 8, (3), 143-155.
- (9) Yoshikawa, H. Y.; Murai, R.; Maki, S.; Kitatani, T.; Sugiyama, S.; Sasaki, G.; Adachi, H.; Inoue, T.; Matsumura, H.; Takano, K.; Murakami, S.; Sasaki, T.; Mori, Y., Laser energy dependence on femtosecond laser-induced nucleation of protein. *Appl. Phys. A* **2008**, 93, (4), 911-915.
- (10) Yoshikawa, H. Y.; Murai, R.; Sugiyama, S.; Sasaki, G.; Kitatani, T.; Takahashi, Y.; Adachi, H.; Matsumura, H.; Murakami, S.; Inoue, T.; Takano, K.; Mori, Y., Femtosecond laser-induced nucleation of protein in agarose gel. *J. Cryst. Growth* **2009**, 311, (3), 956-959.
- (11) Murai, R.; Yoshikawa, H. Y.; Takahashi, Y.; Maruyama, M.; Sugiyama, S.; Sasaki, G.; Adachi, H.; Takano, K.; Matsumura, H.; Murakami, S.; Inoue, T.; Mori, Y., Enhancement of femtosecond laser-induced nucleation of protein in a gel solution. *Appl. Phys. Lett.* **2010**, 96, (4), 043702.

- (12) Murai, R.; Yoshikawa, H. Y.; Hasenaka, H.; Takahashi, Y.; Maruyama, M.; Sugiyama, S.; Adachi, H.; Takano, K.; Matsumura, H.; Murakami, S.; Inoue, T.; Mori, Y., Influence of energy and wavelength on femtosecond laser-induced nucleation of protein. *Chem. Phys. Lett.* **2011**, 510, (1-3), 139-142.
- (13) Sugiyama, T.; Masuhara, H., Laser-Induced Crystallization and Crystal Growth. *Chem. Asian J.* **2011**, 6, (11), 2878-2889.
- (14) Fisher, A.; Pagni, R. M.; Compton, R. N.; Kondepudi, D., In *Nanoclusters: A bridge across disciplines*, Jena, P.; Castleman Jr, A. W., Eds. Elsevier: Amsterdam, 2010; Vol. 1, pp 329-350.
- (15) Sugiyama, T.; Adachi, T.; Masuhara, H., Crystallization of Glycine by Photon Pressure of a Focused CW Laser Beam. *Chem. Lett.* **2007**, 36, 1480.
- (16) Masuhara, H.; Sugiyama, T.; Rungsimanon, T.; Yuyama, K.-i.; Miura, A.; Tu, J.-R., Laser-trapping assembling dynamics of molecules and proteins at surface and interface. *Pure Appl. Chem.* **2011**, 83, (4), 869-883.
- (17) Yuyama, K.-i.; Rungsimanon, T.; Sugiyama, T.; Masuhara, H., Selective Fabrication of alpha- and gamma-Polymorphs of Glycine by Intense Polarized Continuous Wave Laser Beams. *Cryst. Growth Des.* **2012**, 12, (5), 2427-2434.
- (18) Yuyama, K.-i.; Rungsimanon, T.; Sugiyama, T.; Masuhara, H., Formation, Dissolution, and Transfer Dynamics of a Millimeter-Scale Thin Liquid Droplet in Glycine Solution by Laser Trapping. *J. Phys. Chem. C* **2012**, 116, (12), 6809-6816.
- (19) Sugiyama, T.; Adachi, T.; Masuhara, H., Crystal Growth of Glycine Controlled by a Focused CW Near-infrared Laser Beam. *Chem. Lett.* **2009**, 38, (5), 482-483.
- (20) Rungsimanon, T.; Yuyama, K.; Sugiyama, T.; Masuhara, H., Crystallization in Unsaturated Glycine/D2O Solution Achieved by Irradiating a Focused Continuous Wave Near Infrared Laser. *Cryst. Growth Des.* **2010**, 10, (11), 4686-4688.
- (21) Rungsimanon, T.; Yuyama, K.; Sugiyama, T.; Masuhara, H.; Tohnai, N.; Miyata, M., Control of Crystal Polymorph of Glycine by Photon Pressure of a Focused Continuous Wave Near-Infrared Laser Beam. *J. Phys. Chem. Lett.* **2010**, 1, (3), 599-603.
- (22) Uwada, T.; Fujii, S.; Sugiyama, T.; Usman, A.; Miura, A.; Masuhara, H.; Kanaizuka, K.; Haga, M.-a., Glycine Crystallization in Solution by CW Laser-Induced Microbubble on Gold Thin Film Surface. *ACS Appl. Mater. Interfaces* **2012**, 4, (3), 1158-1163.

- (23) Garetz, B. A.; Aber, J. E.; Goddard, N. L.; Young, R. G.; Myerson, A. S., Nonphotochemical, polarization-dependent, laser-induced nucleation in supersaturated aqueous urea solutions. *Phys. Rev. Lett* **1996**, 77, (16), 3475-3476.
- (24) Alexander, A. J.; Camp, P. J., Single Pulse, Single Crystal Laser-Induced Nucleation of Potassium Chloride. *Cryst. Growth Des.* **2009**, 9, (2), 958-963.
- (25) Sun, X. Y.; Garetz, B. A.; Myerson, A. S., Supersaturation and polarization dependence of polymorph control in the nonphotochemical laser-induced nucleation (NPLIN) of aqueous glycine solutions. *Cryst. Growth Des.* **2006**, 6, (3), 684-689.
- (26) Garetz, B. A.; Matic, J.; Myerson, A. S., Polarization switching of crystal structure in the nonphotochemical light-induced nucleation of supersaturated aqueous glycine solutions. *Phys. Rev. Lett* **2002**, 89, (17), 175501.
- (27) Zaccaro, J.; Matic, J.; Myerson, A. S.; Garetz, B. A., Nonphotochemical, laser-induced nucleation of supersaturated aqueous glycine produces unexpected gamma-polymorph. *Cryst. Growth Des.* **2001**, 1, (1), 5-8.
- (28) Lee, I. S.; Evans, J. M. B.; Erdemir, D.; Lee, A. Y.; Garetz, B. A.; Myerson, A. S., Nonphotochemical Laser Induced Nucleation of Hen Egg White Lysozyme Crystals. *Cryst. Growth Des.* **2008**, 8, (12), 4255-4261.
- (29) Sun, X. Y.; Garetz, B. A.; Myerson, A. S., Polarization switching of crystal structure in the nonphotochemical laser-induced nucleation of supersaturated aqueous L-histidine. *Cryst. Growth Des.* **2008**, 8, (5), 1720-1722.
- (30) Knott, B. C.; Doherty, M. F.; Peters, B., A simulation test of the optical Kerr mechanism for laser-induced nucleation. *J. Chem. Phys.* **2011**, 134, (15), 154501.
- (31) Ward, M. R.; Copeland, G. W.; Alexander, A. J., Chiral hide-and-seek: Retention of enantiomorphism in laser-induced nucleation of molten sodium chlorate. *J. Chem. Phys.* **2011**, 135, 114508.
- (32) Ward, M. R.; McHugh, S.; Alexander, A. J., Non-photochemical laser-induced nucleation of supercooled glacial acetic acid. *PCCP* **2012**, 14, (1), 90-93.
- (33) Ward, M. R.; Ballingall, I.; Costen, M. L.; McKendrick, K. G.; Alexander, A. J., Nanosecond pulse width dependence of nonphotochemical laser-induced nucleation of potassium chloride. *Chem. Phys. Lett.* **2009**, 481, (1-3), 25-28.

- (34) Duffus, C.; Camp, P. J.; Alexander, A. J., Spatial Control of Crystal Nucleation in Agarose Gel. *J. Am. Chem. Soc.* **2009**, 131, (33), 11676-11677.
- (35) Knott, B. C.; Larue, J. L.; Wodtke, A. M.; Doherty, M. F.; Peters, B., Bubbles, crystals, and laser-induced nucleation. *J. Chem. Phys.* **2011**, 134, (17), 171102.
- (36) Karpov, V. G., Electric field driven optical recording. *Appl. Phys. Lett.* **2010**, 97, (3), 033505.
- (37) Nardone, M.; Karpov, V. G., Nucleation of metals by strong electric fields. *Appl. Phys. Lett.* **2012**, 100, (15), 151912.
- (38) In *CRC Handbook of Chemistry and Physics*, 91st (Internet Version 2011) ed.; Haynes, W. M., Ed. CRC Press: Boca Raton, FL, 2011.
- (39) Matic, J.; Sun, X. Y.; Garetz, B. A.; Myerson, A. S., Intensity, wavelength, and polarization dependence of nonphotochemical laser-induced nucleation in supersaturated aqueous urea solutions. *Cryst. Growth Des.* **2005**, 5, (4), 1565-1567.
- (40) Mersmann, A., Calculation of interfacial tensions. *J. Cryst. Growth* **1990**, 102, 841-847.
- (41) Nielsen, A. E.; Söhnel, O., Interfacial Tensions Electrolyte Crystal-Aqueous Solution, from Nucleation Data. *J. Cryst. Growth* **1971**, 11, 233.
- (42) Kashchiev, D.; van Rosmalen, G. M., Review: Nucleation in solutions revisited. *Crystal Research and Technology* **2003**, 38, (7-8), 555-574.
- (43) Cohen, M. D.; Flagan, R. C.; Seinfeld, J. H., Studies of concentrated electrolyte solutions using the electrodynamic balance. 3. Solute nucleation. *J. Phys. Chem.* **1987**, 91, (17), 4583-4590.
- (44) Chatterji, A. C.; Singh, R. N., Nucleation from quiet supersaturated solutions of alkali halides. Part I. Potassium and ammonium chlorides, bromides and iodides. *J. Phys. Chem.* **1958**, 62, 1408.
- (45) Erdemir, D.; Lee, A. Y.; Myerson, A. S., Nucleation of Crystals from Solution: Classical and Two-Step Models. *Acc. Chem. Res.* **2009**, 42, (5), 621-629.
- (46) Vekilov, P. G., Nucleation. *Cryst. Growth Des.* **2010**, 10, (12), 5007-5019.
- (47) Vekilov, P. G., Dense liquid precursor for the nucleation of ordered solid phases from solution. *Cryst. Growth Des.* **2004**, 4, 671-685.
- (48) Lechner, W.; Dellago, C.; Bolhuis, P. G., Role of the Prestructured Surface Cloud in Crystal Nucleation. *Phys. Rev. Lett* **2011**, 106, (8), 085701.

- (49) Wolde, P. R.; Frenkel, D., Enhancement of protein crystal nucleation by critical density fluctuations. *Science* **1997**, 277, 1975-1978.
- (50) Lutsko, J. F.; Nicolis, G., Theoretical evidence for a dense fluid precursor to nucleation. *Phys. Rev. Lett.* **2006**, 96, 046102.
- (51) Talanquer, V.; Oxtoby, D. W., Crystal nucleation in the presence of a metastable critical point. *J. Chem. Phys.* **1998**, 109, (1), 223-227.
- (52) Zahn, D., Atomistic mechanism of NaCl nucleation from an aqueous solution. *Phys. Rev. Lett.* **2004**, 92, (4), 040801.
- (53) Chowdhuri, S.; Chandra, A., Molecular dynamics simulations of aqueous NaCl and KCl solutions: Effects of ion concentration on the single-particle, pair, and collective dynamical properties of ions and water molecules. *J. Chem. Phys.* **2001**, 115, (8), 3732-3741.
- (54) Garten, V. A.; Head, R. B., Crystalloluminescence and the Nature of the Critical Nucleus. *Phil. Mag.* **1963**, 8, (95), 1793-1803.
- (55) Garten, V. A.; Head, R. B., Homogeneous Nucleation and the Phenomenon of Crystalloluminescence. *Phil. Mag.* **1966**, 14, 1243-1253.
- (56) Westhaus, U.; Dröge, T.; Sass, R., DETHERM®--a thermophysical property database. *Fluid Phase Equilib.* **1999**, 158-160, 429-435.